

Four-equation turbulence model for prediction of the turbulent boundary layer affected by buoyancy force over a flat plate

MYUNG KYOON CHUNG and HYUNG JIN SUNG

Department of Mechanical Engineering, Korea Advanced Institute of Science and Technology,
Chongryang P.O. Box 150, Seoul, Korea

(Received 28 June 1983 and in final form 25 April 1984)

Abstract—Turbulent convective heat transfer with appreciable buoyancy effect over a heated or cooled horizontal flat plate is numerically analyzed by solving four equations for mean square temperature variance $\overline{\theta^2}$, its rate of destruction ϵ_θ , turbulent kinetic energy k and the rate of kinetic energy dissipation ϵ . Turbulent time-scale ratio R of temperature fluctuations relative to velocity fluctuations defined by $(\overline{\theta^2}/\epsilon_\theta)/(2k/\epsilon)$ is found to vary widely across the boundary layer. For both highly stable and highly unstable conditions, the 'four-equation' model yields better results for mean temperature profile and surface heat flux than the two-equation model. It is also found that the magnitude of thermal von Karman constant κ_θ is not a universal constant but it depends on the thermal stratification of the boundary layer.

INTRODUCTION

A FEW YEARS ago, Launder and Samaraweera [1] applied the second-order turbulence closure model to analyze a flat-plate turbulent boundary layer with a step change in wall heat flux. They have calculated the Reynolds stresses $\overline{u^2}$, $\overline{v^2}$, $\overline{w^2}$, \overline{uv} , the turbulent heat fluxes $\overline{u\theta}$ and $\overline{v\theta}$, and the rate of kinetic energy dissipation ϵ , in addition to mean field variables, such as velocity and temperature. However, such an application of the second-order closure model yielded rather poor prediction of the mean temperature profiles, particularly in the log-law layer, compared to the mixing length model of Browne and Antonia [2]. Discussions about this matter are given in [3] and [4].

Launder and Samaraweera [1] assumed in their formulation of the model equations that the buoyancy effect is negligible and that the thermal time scale ($\tau_\theta = \overline{\theta^2}/\epsilon_\theta$) is proportional to the mechanical time scale ($\tau = k/\epsilon$) which is assumed to be entirely unaffected by the thermal field. They then attributed their prediction inaccuracy to the absence of the characteristic thermal time scale which should be influential on the heat flux process.

When the velocity of the fluid flow is relatively slow or when the vertical heat flux through the wall is comparatively high, turbulence production by buoyancy fluctuation is significant and the diffusive transports of the stress/flux quantities $\overline{u_i u_j}$ and $\overline{u_i \theta}$ depend on the buoyancy, as have been shown theoretically in [5]. The same argument may be extended locally to forced convective heat transfer over a flat plate. In this case, gradient of the mean temperature is large in the region near the wall and the buoyancy fluctuations must be locally very active there, which, in turn, may contribute significantly to the third order diffusive transport of the second order correlations.

One of the buoyancy effects on the thermal field may be represented by the empirical 'constant' κ_θ which measures the inverse of the slope of the log-law mean temperature profile. In an experiment by Subramanian and Antonia [6], where $Rm = 3100$ and $Ri = -3.0 \times 10^{-4}$, the value of κ_θ was shown to be about 0.46. But for a strongly heated boundary layer under the same value of Ri as that of [6], κ_θ is about 0.8 [7]. Note that in this case the Reynolds number is very small, $Rm = 293$. Arya's [8] experiments on the buoyancy effects in a horizontal flat plate boundary layer show that the value of κ_θ varies between 0.41 and 0.77 with the lower value for more stable condition. Petukhov *et al.* [9] showed that mean temperature and mean velocity profiles, coefficients of friction and heat transfer, turbulent intensity, Reynolds shear stress and heat flux are shown to be strongly dependent on thermal stratification.

Gibson and Launder [10, 11] have formulated an extended k - ϵ model, the so called algebraic stress/flux models, which include appropriate buoyancy terms in the models for \overline{uv} , $\overline{v^2}$ and $\overline{v\theta}$ which are functions of $\partial U/\partial y$, $\partial T/\partial y$, k and ϵ . Gibson and Launder [10] proposed to include transport equations for $\overline{\theta^2}$ and ϵ_θ but, due to inadequate information about the model equation for ϵ_θ , they approximated $\overline{\theta^2}$ in their actual computations by assuming a constant time scale ratio, $R = 0.8$ (the same method was adopted in Rodi [12] and Ljuboja and Rodi [13]). Lin and Lin [14] and Warhaft and Lumley [15] observed experimentally that the value of R varies between 0.4 and 1.5 even in a grid-generated homogeneous scalar field. Re-evaluation of data in various kinds of non-isothermal shear flows compiled in [16] shows that R varies between 0.35 and 0.6 with its mean of about 0.5.

In this paper, an attempt is made to clarify problems inherent in the k - ϵ model mentioned above; namely, the inability to supply a necessary turbulent thermal time scale and the weakness in taking full account of the

NOMENCLATURE			
B_q	dissipation model constant	x, y, z	coordinates
f	wall damping function, equation (28)	y^+	dimensionless wall distance = $u_* y/\nu$.
G	rate of buoyancy production of turbulent kinetic energy = $-\beta g \overline{v\theta}$	Greek symbols	
g	gravitational acceleration		
k	turbulent kinetic energy = $\frac{1}{2}(\overline{u^2} + \overline{v^2} + \overline{w^2})$	α	fluid thermal diffusivity
l	mixing length	α_t	turbulent eddy diffusivity
P	rate of shear production of turbulent kinetic energy = $-\overline{u\bar{v}} \partial U/\partial y$	β	volumetric expansion coefficient
Q_w	thermometric wall heat flux	δ	boundary layer thickness
R	ratio of time scales = $\tau_\theta/2\tau$	δ_2	momentum thickness
Re	Reynolds number = $U_\infty \delta/\nu$	ε	rate of dissipation of turbulent kinetic energy
R_f	flux Richardson number = $-G/P$	ε_θ	rate of destruction of $\overline{\theta^2}$
Ri	gradient Richardson number = $-\beta g(\partial T/\partial y)/(\partial U/\partial y)^2$	κ	von Karman constant
	or bulk Richardson number = $-g\delta\Delta T/T_0 U_\infty^2$	ν	kinematic molecular viscosity
Rm	momentum thickness Reynolds number = $U_\infty \delta_2/\nu$	ν_t	eddy viscosity $\equiv -\overline{u\bar{v}}/(\partial U/\partial y)$
T	mean temperature	ρ	fluid density
T_*	friction temperature = Q_w/u_*	$\overline{\theta^2}$	mean square temperature variance
ΔT	potential temperature difference across the boundary layer	τ	mechanical time scale = k/ε
U, V	mean velocity components	τ_θ	thermal time scale = $\overline{\theta^2}/\varepsilon_\theta$
u_*	friction velocity = $\sqrt{\tau_w/\rho}$	σ_t	turbulent Prandtl number.
u', v', w'	r.m.s. velocity fluctuations in x -, y -, z -directions	Subscripts	
		c	value at the matching point
		o	non-buoyant or reference
		t	turbulent
		w	wall
		∞	ambient.

buoyancy effects by the simple gradient models for third-order transport terms.

The objective of the present paper is to resolve these problems by a four-equation model which includes transport equations for $\overline{\theta^2}$ and ε_θ in addition to k and ε . The proposed set of equations is then applied to the simulation of a few experiments on the convective heat transfer over horizontal flat plates with varying degrees of buoyancy. For comparison, the k - ε equations with algebraic stress/flux models are also applied to the simulation.

FOUR-EQUATION MODEL

Governing equations for the mean velocity and the temperature for a two-dimensional thin boundary layer flow over a horizontal flat plate under the Boussinesq approximation are as follows:

$$\frac{\partial(\rho U)}{\partial x} + \frac{\partial(\rho V)}{\partial y} = 0$$

(1)

$$\rho U \frac{\partial U}{\partial x} + \rho V \frac{\partial U}{\partial y} = \frac{\partial}{\partial y} \left(\mu \frac{\partial U}{\partial y} - \rho \overline{u\bar{v}} \right)$$

(2)

$$\rho U \frac{\partial T}{\partial x} + \rho V \frac{\partial T}{\partial y} = \frac{\partial}{\partial y} \left(\rho \alpha \frac{\partial T}{\partial y} - \rho \overline{v\theta} \right)$$

(3)

$$\rho = \rho(T).$$

(4)

Since the mean pressure does not change in the flow field, the air density is a function of the mean temperature only. Hence, the interpolation formula for the density given by Holman [17] is useful for our purpose. Model equations for Reynolds stresses $\overline{u_i u_j}$ and turbulent heat flux $\overline{u_i \theta}$ have been well documented at the truncated second-order closure level in for example, [10] and they are as follows:

$$\frac{\overline{u\bar{v}}}{k} = \frac{1 - C_2 + \frac{3}{2}C_2 C_2' f}{C_1 + \frac{3}{2}C_1' f} \frac{\overline{v^2}}{\varepsilon} \frac{\partial U}{\partial y} - \frac{1 - C_3}{C_1 + \frac{3}{2}C_1' f} \beta g \frac{\overline{u\bar{\theta}}}{\varepsilon}$$

(5)

$$\frac{\overline{v^2}}{k} = \frac{2}{3} \frac{C_1 - 1 + \frac{P + G}{\varepsilon} (C_2 - 2C_2 C_2' f) + \frac{G}{\varepsilon} (3 - C_2 - 2C_3 + 2C_2 C_2' f)}{C_1 + 2C_1' f + \frac{P + G}{\varepsilon} - 1}$$

(6)

$$\frac{\overline{u^2}}{k} = \frac{C_1 f \frac{\overline{v^2}}{k} + \frac{2}{3} \left[C_1 - 1 + \frac{P+G}{\varepsilon} (3 - 2C_2 + C_2 C_2' f) + \frac{G}{\varepsilon} (C_3 - 3 + 2C_2 - C_2 C_2' f) \right]}{C_1 - 1 + \frac{P+G}{\varepsilon}} \quad (7)$$

$$-\overline{u\theta} = \frac{1}{C_{1\theta}} \frac{k}{\varepsilon} \overline{uv} \frac{\partial T}{\partial y} + \frac{1 - C_{2\theta}}{C_{1\theta}} \frac{k}{\varepsilon} \overline{v\theta} \frac{\partial U}{\partial y} \quad (8)$$

$$-\overline{v\theta} = \frac{1}{C_{1\theta} + C_{1\theta}' f} \frac{k}{\varepsilon} \overline{v^2} \frac{\partial T}{\partial y} - \frac{1 - C_{3\theta}}{C_{1\theta} + C_{1\theta}' f} \frac{k}{\varepsilon} \beta g \overline{\theta^2} \quad (9)$$

where, C_s are model constants whose values are adopted from [13] as shown in Table 1, and function f is a wall function which will be explained later. Model equations (5), (8) and (9) are obtained under the assumption of local equilibrium state such that convective transport of a related second-order quantity is perfectly balanced by the diffusive transport and thus the production (or source) term becomes equal to the dissipation (or sink) term. Equations (6) and (7) were, however, derived more generally for non-equilibrium condition in order to keep certain consistency between the magnitudes of $\overline{v^2}$ and k ; the latter value is obtained by solving its non-equilibrium transport equation

for horizontally homogeneous buoyant convection has been successfully used by Zeman and Lumley [20].

Newman *et al.* [21] have carefully examined available experimental data on evolution process of $\overline{\theta^2}$ in homogeneous flows, with and without mean temperature gradients, and have formulated an approximate transport equation which contains two sink terms, one of which responds to the time scale of the velocity field while the other reflects that of the scalar field itself. In addition, a production term due to the heat flux anisotropy and the temperature gradient is included in the model equation for flows with a mean scalar gradient.

Following the same line of thought, it is thought that, when the mean shear is present in the flow field, a 'production' term due to increase of turbulent kinetic energy by the mean shear and the buoyancy must also appear in the equation. Thus, our model equation for ε_θ is given by the following form:

$$U \frac{\partial \varepsilon_\theta}{\partial x} + V \frac{\partial \varepsilon_\theta}{\partial y} = \frac{\partial}{\partial y} [-\varepsilon_\theta \overline{v}] - 0.8 \frac{\varepsilon \varepsilon_\theta}{k} - 2.0 \frac{\varepsilon_\theta^2}{\overline{\theta^2}} - 1.96 \frac{\varepsilon_\theta}{\overline{\theta^2}} \overline{v\theta} \frac{\partial T}{\partial y} + C_b (P + G) \frac{\varepsilon_\theta}{k} \quad (13)$$

(sink at τ) (sink at τ_θ) ('production' of ε_θ due to $\overline{v\theta} \partial T / \partial y$) ('production' of ε_θ due to $P + G$)

(Ljuboja and Rodi [13]). Now, our system of equations from (1) to (9) is supplemented by the following transport equations for k , ε and $\overline{\theta^2}$ as follows [12]:

$$U \frac{\partial k}{\partial x} + V \frac{\partial k}{\partial y} = \frac{\partial}{\partial y} [-\overline{kv}] - \overline{uv} \frac{\partial U}{\partial y} + \beta g \overline{v\theta} - \varepsilon \quad (10)$$

$$U \frac{\partial \varepsilon}{\partial x} + V \frac{\partial \varepsilon}{\partial y} = \frac{\partial}{\partial y} [-\varepsilon \overline{v}] - C_{\varepsilon 1} \times \frac{\varepsilon}{k} \overline{uv} \frac{\partial U}{\partial y} - C_{\varepsilon 1} \frac{\varepsilon}{k} (1 - C_{\varepsilon 3}) \beta g \overline{v\theta} - C_{\varepsilon 2} \frac{\varepsilon^2}{k} \quad (11)$$

$$U \frac{\partial \overline{\theta^2}}{\partial x} + V \frac{\partial \overline{\theta^2}}{\partial y} = \frac{\partial}{\partial y} [-\overline{\theta^2} \overline{v}] - 2\overline{v\theta} \frac{\partial T}{\partial y} - 2\varepsilon_\theta \quad (12)$$

For completeness, a transport equation for the rate of scalar dissipation ε_θ is also needed. Its exact transport equation has been discussed by Launder [18]. A tentative model equation for non-isothermal shear flows has been formulated using the tensor invariant modeling by Lumley [19] and its simplified equation

The first three constants in the equation (13) are taken from Newman *et al.* [21] and the last constant C_b has been selected as $C_b = 0.8$ in order to exhibit the state of equilibrium.

Recently, Pope [22] showed that, for homogeneous flows without mean gradient, consistency condition does not admit the third term in the right-hand side of equation (13). Instead, he showed that a term like $\overline{\theta^2} \varepsilon^2 / k^2$ should be included. Adoption of Pope's model equation together with 'production' terms in equation (13) requires knowledge of values of three more model constants, which is presently difficult to obtain. Therefore, tentatively, the equation (13) is adopted in the present computation.

Now, some discussions about the third order transport terms (\overline{kv} , $\overline{v\theta}$, $\overline{\theta^2 v}$ and $\overline{\varepsilon_\theta v}$) are in order. If we define the eddy viscosity ν_t in the conventional manner, it can be easily derived from equations (5)–(9) as a function of k , ε , f and the buoyancy $\beta g \frac{\partial T}{\partial y}$ [13]. Then, the simple gradient transport models for \overline{kv} and $\overline{v\theta}$ are written in terms of ν_t as follows [11]:

$$\overline{kv} = -\frac{\nu_t}{\sigma_k} \frac{\partial k}{\partial y} \quad (14)$$

$$\overline{v\theta} = -\frac{\nu_t}{\sigma_\varepsilon} \frac{\partial \varepsilon}{\partial y} \quad (15)$$

Table 1. Constants in the turbulence model

$C_1 = 1.8$	$C_1' = 0.6$	$C_2 = 0.6$	$C_2' = 0.3$
$C_3 = 0.6$	$C_{1\theta} = 3.0$	$C_{2\theta} = 0.5$	$C_{3\theta} = 0.5$
$C_{1\theta}' = 0.5$	$\sigma_k = 1.0$	$\sigma_\varepsilon = 1.3$	$C_{\varepsilon 1} = 1.44$
$C_{\varepsilon 2} = 1.92$	$C_{\varepsilon 3} = 0.8$	$C_w = 3.72$	$R = 0.8$

where σ_k and σ_ϵ are model constants of order one. So far, the buoyancy effects have been incorporated in our model equations through the pressure strain correlation models and through the explicit buoyancy production terms. According to Zeman [23], the buoyancy contributions to the third-order transports are significant in non-isothermal turbulent flows. However, since the models (5), (7), (9) have been derived by dropping the third-order transport terms, such contributions have been largely neglected in the models (14) and (15).

Detailed form of v_t [13] shows that it does not explicitly contain mean shear. Rather, it is seen to be strongly dependent on the buoyancy. Assuming that the third-order transports of $\bar{\theta}^2$ and ϵ_θ are even less dependent on the mean shear than k and ϵ , Zeman and Lumley's [20] buoyancy transport models for the mixed layer caused by buoyancy may be applied to our problem as follows:

$$\overline{\partial^2 v} = -K_t \frac{\partial \bar{\theta}^2}{\partial y} \quad (16)$$

$$\overline{\epsilon_\theta v} = -0.5 K_t \frac{\partial \epsilon_\theta}{\partial y} + 0.5 \beta g \tau_c \left(K_t \frac{\partial T}{\partial y} - \bar{v} \bar{\theta} \right) \frac{\partial \bar{\theta}^2}{\partial y} \quad (17)$$

where

$$K_t = \tau_c (\bar{v}^2 + 0.6 \beta g \bar{v} \bar{\theta} \tau_c) \left(1 + 0.1 \tau_c \theta_\theta \beta g \left| \frac{\partial T}{\partial y} \right| \right) \quad (18)$$

and

$$\tau_c = \left(\frac{3.5}{\tau} + \frac{2}{\tau_\theta} \right)^{-1} \quad (19)$$

where K_t is an eddy coefficient for the third-order transport of $\bar{\theta}^2$ and τ_c is a composite time scale.

The above four-equation model can be shown to be simplified to the two-equation model with the application of the appropriate model [10].

$$\bar{\theta}^2 = -2R \frac{k}{\epsilon} \bar{v} \bar{\theta} \frac{\partial T}{\partial y} \quad (20)$$

where the time scale ratio is held constant at $R = 0.8$ as in [10] and [12].

BOUNDARY CONDITIONS AND NUMERICAL METHOD

The turbulence model equations introduced above are formulated under the assumption of high turbulent Reynolds numbers and thus are not valid for the viscous sublayer very close to the wall. The usual practice to overcome this problem is to introduce a wall-layer matching procedure in which the mean velocity and the mean temperature profiles are first calculated up to a certain point y_c^+ , not far from the wall, by an appropriate mixing-length model and then the high Reynolds number turbulence models are applied from

the point y_c^+ as a lower boundary to the free boundary. The matching point y_c^+ is usually selected in the region $30 \leq y^+ \leq 50$, where the turbulence is assumed to be in an equilibrium state, i.e. production and dissipation of turbulent kinetic energy are approximately in balance. In addition, this region is characterized as a constant stress layer where $-\bar{u}\bar{v} = u_*^2$ and the mean velocity profile starts to follow the logarithmic law of the wall.

The mixing-length model used in the wall region $0 \leq y^+ \leq y_c^+$ is that of Panofsky [24] for unstable condition ($Ri < 0$),

$$l = l_0(1 - 14 Ri)^{-1/4} \quad (21)$$

or that of Monin–Oboukhov relation for stable condition ($Ri > 0$),

$$l = l_0(1 - 7 Ri) \quad (22)$$

where l_0 is the mixing length given by van Driest [25]. The mean temperature profile in the wall region is calculated by introducing the following Munk–Anderson formula [12] which takes into account the buoyancy effect by Ri :

$$\sigma_t = \sigma_{t0}(1 + 3.33 Ri)^{1.5}/(1 + 10 Ri)^{0.5} \quad (23)$$

where σ_{t0} is the non-buoyant turbulent Prandtl number which is considered variable dependent on the eddy viscosity [25].

In order to match the mean velocity profiles smoothly at the matching point, the eddy viscosity v_t is selected as a matching parameter, i.e. $v_{t, \text{below}} = v_{t, \text{above}}$ at y_c^+ . This requirement yields the following lower boundary values for k_c and ϵ_c :

$$k_c = \left(\frac{B_q}{C_\mu} \right)_c^2 \left(\kappa l \left| \frac{\partial U}{\partial y} \right|_c \right)^2; \quad \epsilon_c = (B_q \kappa) k_c^{3/2} / l_c \quad (24)$$

where κ is the von Karman constant and B_q is a dissipation model constant, $B_q = 0.4$. The value of $(C_\mu)_c$ is determined by a relation

$$(-\bar{u}\bar{v})_c \equiv \left(v_t \frac{\partial U}{\partial y} \right)_c \approx \left(C_\mu \frac{k^2}{\epsilon} \frac{\partial U}{\partial y} \right)_c,$$

where $-\bar{u}\bar{v}$ is formulated in (5). Note that $(C_\mu)_c$ depends on the wall-damping function f and buoyancy. Since it is known that $\sigma_t \approx 1$ in turbulent boundary layer, the momentum thickness is assumed to be the same as the thermal boundary-layer thickness in the flat plate boundary layer flow. With this assumption, the local equilibrium matching point of the thermal field is also taken to be y_c^+ . The boundary conditions of $\bar{\theta}_c^2$ and $\epsilon_{\theta c}$ are

$$\begin{aligned} \bar{\theta}_c^2 &= 2R \frac{(C_\mu)_c}{\sigma_{t,c}} k_c^3 \left(\frac{\partial T}{\partial y} \right)_c^2; \\ \epsilon_{\theta c} &= \frac{(C_\mu)_c}{\sigma_{t,c}} \frac{k_c^2}{\epsilon_c} \left(\frac{\partial T}{\partial y} \right)_c^2 \end{aligned} \quad (25)$$

where $\sigma_{t,c}$ is the turbulent Prandtl number computed from (23) at y_c^+ .

The wall function in (5)–(9) which was first introduced by Daly and Harlow [26] to take into

account wall proximity effect by pressure fluctuations on the transfer of kinetic energy between components has been used in various forms [10, 13, 26, 27]. The lower boundary values k_c and ε_c estimated from the region above the matching point y_c^+ are easily seen to be

$$k_c = \sqrt{\frac{1-R_f}{C_\mu}} u_*^2; \quad \varepsilon_c = \frac{u_*^3}{\kappa y_c} (1-R_f). \quad (26)$$

These values are found to be within $\pm 3\%$ difference compared to the values by (24) which are estimated from the wall region. According to Daly and Harlow [26], f is assumed to be proportional to l/y and $l \sim k^{3/2}/\varepsilon$. Thus, we have,

$$f = ak^{3/2}/\varepsilon. \quad (27)$$

Since the function f has to be unity at the matching point y_c^+ [10, 13], substitution of (26) into the function f gives the proportionality constant, $a = c'(1-R_f)^{1/4}$. Thus,

$$f = \frac{k^{3/2}}{C_w y \varepsilon} (1-R_f)^{1/4}. \quad (28)$$

This wall function differs from Ljuboja and Rodi [13] by the buoyancy correction factor $(1-R_f)^{1/4}$.

For numerical computations, Patankar–Spalding's marching forward scheme [25] has been used. Computations were started at the leading edge with finitely thin δ whose velocity profile is that of one-seventh power law. Initial profiles of turbulent variables were assumed to be same as those in fully developed boundary layer of appropriate magnitudes. It was found that the computed profiles far downstream are not dependent on the estimated initial profiles.

COMPUTATIONAL RESULTS AND DISCUSSIONS

In order to test the universal validity of our computational models, development of a turbulent boundary layer over a heated or cooled flat plate maintained at a constant plate temperature or at a constant heat flux was simulated and compared with available experimental data reported by different authors. The experiments of Subramanian and Antonia (henceforth designated by SA) [6] were carried out to investigate the effect of Reynolds number on a turbulent boundary layer over a slightly heated flat plate with a uniform heat flux, hence their conditions are closest to those of neutral stability among the experiments tested in the present study. Cheng and Ng's experiment [7] was performed at the same Ri as SA but at much lower Rm with a constant wall temperature condition. Arya's data [8] were taken under both stable and unstable conditions of the flat plate maintained at a constant temperature in a long wind tunnel. For the case of Perry and Hoffmann's [28] constant wall-temperature experiments, the mean temperature profile was not reported and thus only data of temperature fluctuations can be used to compare with results of the

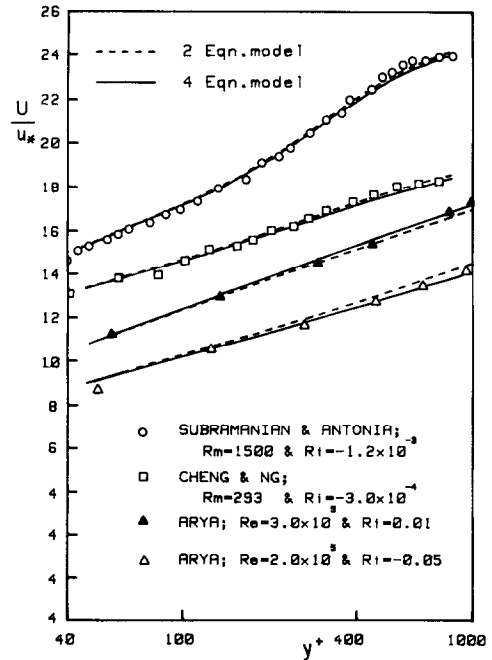


FIG. 1. Mean velocity profiles in flat plate boundary layer. ---, ——— Calculations; \circ , \square , \triangle , \blacktriangle , experiments.

present study. Data of the mean velocity and the mean temperature reported in the above four studies show well-defined mean field profiles and no experimental uncertainties were given in these papers. However, experimental uncertainties on the turbulent correlations $\overline{u'v'}$ and $\overline{v'\theta}$ and the turbulent kinetic energy k were: $\pm 7\%$ in SA, $\pm 12\%$ in Cheng and Ng and ± 10 – 15% in Arya.

We first present the mean field profiles in the turbulent boundary layer. Figure 1 shows comparison of mean velocity profiles by experiments with those by computation using both models. The solid line indicates the computed profiles by the four-equation model and the dotted lines show results by the two-equation model. For the case of SA, the two computational methods yield complete agreement with experimental data. Both models yield correct variation of the logarithmic slope showing the dependency on the thermal stability.

The mean temperature profiles are compared in Fig. 2. The slope of the profiles is very sensitive to the stability. For the stable case (\blacktriangle), κ_θ takes a value of about 0.45, but for the unstable case (\triangle), $\kappa_\theta \approx 0.70$. The two-equation model underpredicts the mean temperatures for the stable condition and overpredicts them for the unstable conditions. However, the four-equation model properly predicts the variation of the mean temperature profiles depending on the stability conditions.

Shown in Fig. 3 are the turbulent Reynolds shear stress profiles. Since the buoyancy effect is not dominant in SA, the two models yield almost identical results. It can be seen that the wall cooling causes a

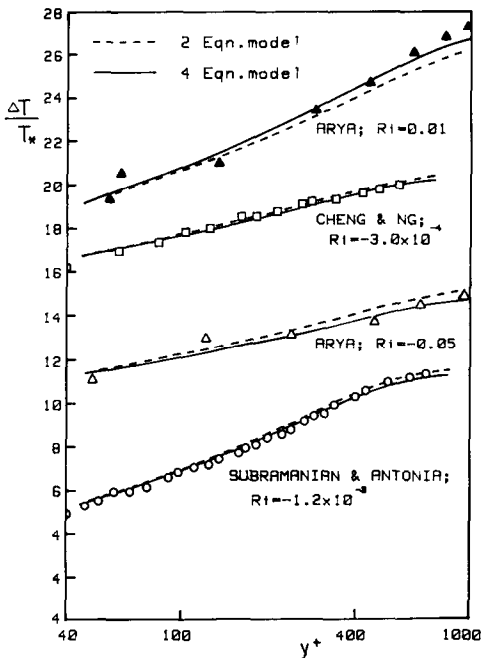


FIG. 2. Mean temperature profiles in flat plate boundary layer. Symbols representing data are the same as in Fig. 1.

reduction of $-\overline{uv}/U_\infty^2$ and the wall heating an increase, in agreement with experimental observations [8]. Note that $-\rho\overline{uv}/\rho_\infty u_\infty^2$ has lower value than that of unheated boundary layer due to the fact that $-\rho\overline{uv}/\rho_\infty u_\infty^2 \leq 1$ and $\rho_\infty/\rho_w > 1$ in the unstable boundary layer as can be seen in [7]; therefore, Cheng and Ng's assertion that the wall heating causes reduction in Reynolds stress $-\rho\overline{uv}$ is also verified.

The vertical heat flux profiles are shown in Fig. 4. As can be seen in the figure, predicted values by both models are higher than the experimental values in the whole region; but, the shape of the profile of the turbulent heat flux is in general agreement between the predicted and the measured values. Also shown in the figure is the effect of Ri on the variation of the vertical heat flux. When the thermal field becomes more stable, the profile of the nondimensional vertical heat flux shifts downward as the case of the Reynolds shear stress.

Figure 5 shows the intensity $(\sqrt{\theta^2})/T_*$ of temperature fluctuations. All curves represent predicted profiles by the four-equation model and are in reasonably good agreements with experimental data. It can be seen in the figure that the value $(\sqrt{\theta^2})/T_*$ is lower for more unstable condition [29].

The skin friction and the surface heat flux are presented as a function of Ri in Fig. 6. Both models yield satisfactory results which are in good agreement with the data in both stable and unstable conditions. The difference between the results by the two models may be within the experimental error. However, the four-equation model consistently gives better results, especially for higher $|Ri|$, by more than 5%.

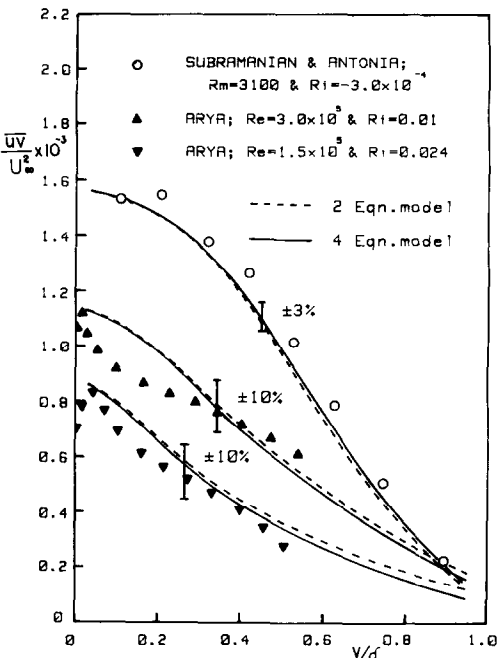


FIG. 3. Distributions of the Reynolds shear stress under stable and unstable conditions. ---, — Calculations; ○, ▲, ▼ experiments.

The subject of evolution of the time scale ratio R has recently been discussed by Pope [22]. He mentions that the value of R is observed experimentally in the range of $0.4 < R < 1.7$ depending upon the initial conditions and that R remains constant as the turbulence decays, rather than relaxing to an equilibrium value. Figure 7

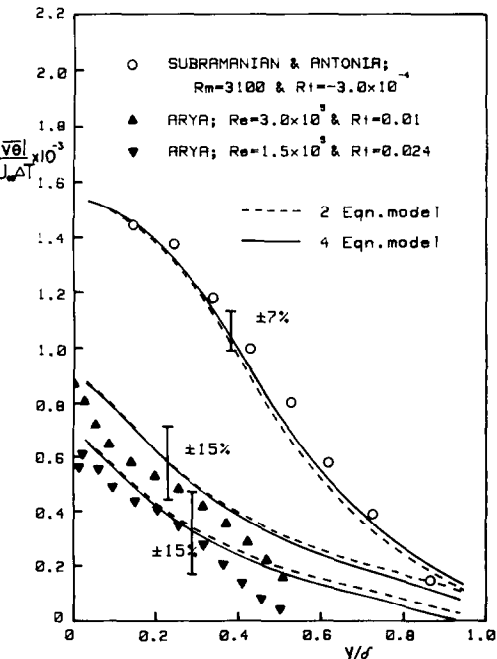


FIG. 4. Distributions of the vertical heat flux under stable and unstable conditions. ---, — Calculations; ○, ▲, ▼ experiments.

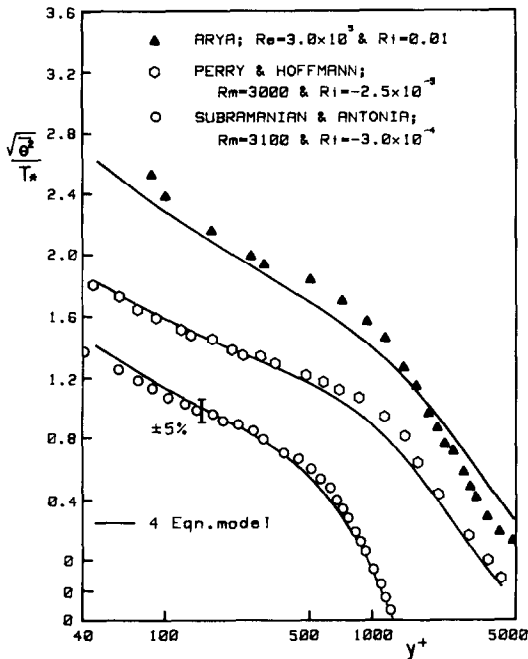


FIG. 5. Distributions of r.m.s. temperature under stable and unstable conditions. — Calculations; ▲, ○, ○ experiments.

shows calculated variations of R across the boundary layer under different stratifications. Rough estimation of R by Béguier *et al.* [16] using Fulachier’s data on heated flat plates shows similar variation as in Fig. 7, but smaller magnitude of about 0.37–0.6. Since most of the model constants in Table 1 were selected under the assumption that $R = 0.8$, initial matching value R_c at the matching point was taken as 0.8 in our computation. It is not yet clear why smaller value R_c of about 0.5 in accordance with [16] causes oscillation of R profile at the downstream finally reaching to unreasonably high value of $R > 2$. An important observation from Fig. 7 is that, when the thermal stratification of the boundary layer is far from the

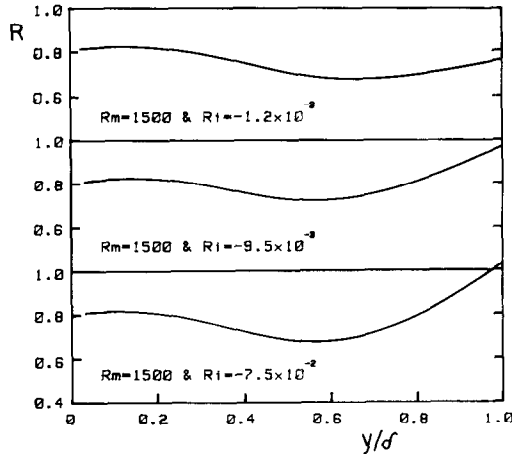


FIG. 7. Computed variations of the time scale ratio R across the boundary layer under unstable conditions.

neutral condition, the variation of R is substantial across the boundary layer.

CONCLUSIONS

A four-equation turbulence model is presented to predict flows with a large buoyancy effect. The main merit of the four-equation model is to introduce the variable time scale ratio R which depends on the thermal stratification. Assuming that the third-order diffusive transport terms in transport equations for θ^2 and ε_θ are predominantly dependent on the buoyancy, the buoyancy transport models of Zeman and Lumley [20] were adopted in this study. The wall damping function, which takes into account the wall proximity effect by the pressure fluctuations on the transfer of energy among components, is used as a function of distance and the local flux Richardson number.

It is found that when the thermal stratification is not far from neutral stability, the four-equation model and the two-equation model yield similar results; differences are negligible from the engineering point of view. However, if the buoyancy effect is strong both in positive and negative directions, the four-equation model yields more accurate results on the mean temperature profile and the surface heat flux. Through our computations and survey of the experimental data, an important observation has been made; the von Karman ‘constants’ in logarithmic representations of mean temperature as well as mean velocity profiles are not really constant as have usually been thought to be, but, rather depend on the relative magnitude between Rm and Ri . The effects of buoyancy forces are such that increasing instability results in reduction of Reynolds shear stress and nondimensional temperature fluctuations $(\sqrt{\theta^2})/T_*$. Furthermore, nondimensional skin friction and surface heat flux, u_*/U_∞ and $T_*/\Delta T$, decrease with increasing stability. The time scale ratio R is seen to vary widely across the boundary layer due to strong buoyancy forces.

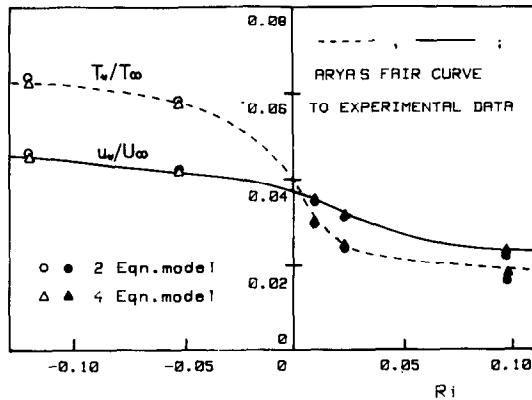


FIG. 6. Distributions of the friction and heat transfer under stable and unstable conditions. ○, ●, △, ▲ Calculations; ---, — experiments.

REFERENCES

1. B. E. Launder and D. S. A. Samaraweera, Application of a second-moment turbulence closure to heat and mass transport in thin shear flow—I. Two-dimensional transport, *Int. J. Heat Mass Transfer* **22**, 1631–1643 (1979).
2. L. W. B. Browne and R. A. Antonia, Calculation of a turbulent boundary layer downstream of a step change in surface temperature, *J. Heat Transfer* **101**, 144–150 (1979).
3. R. A. Antonia, Discussion of “Application of a second-moment turbulence closure to heat and mass transport in thin shear flow—I. Two-dimensional transport”, *Int. J. Heat Mass Transfer* **24**, 1747 (1981).
4. B. E. Launder, Author’s response to “Application of a second-moment turbulence closure to heat and mass transport in thin shear flows”, *Int. J. Heat Mass Transfer* **24**, 1748 (1981).
5. J. L. Lumley, O. Zeman and J. Siess, The influence of buoyancy on turbulent transport, *J. Fluid Mech.* **84**, 581–597 (1978).
6. C. S. Subramanian and R. A. Antonia, Effect of Reynolds number on a slightly heated turbulent boundary layer, *Int. J. Heat Mass Transfer* **24**, 1833–1846 (1981).
7. R. K. Cheng and T. T. Ng, Some aspects of strongly heated turbulent boundary layer flow, *Physics Fluids* **25**, 1333–1341 (1982).
8. S. P. S. Arya, Buoyancy effects in a horizontal flat plate boundary layer, *J. Fluid Mech.* **68**, 321–343 (1975).
9. B. S. Petukhov, A. F. Polyakov and Yu. V. Tsypulev, Peculiarities of non-isothermal turbulent flow in horizontal flat channel at low Reynolds number and under significant influence of buoyancy forces, 2nd Symposium on Turbulent Shear Flow, 9, pp. 11–16, Imperial College, London (1979).
10. M. P. S. Gibson and B. E. Launder, Ground effects on pressure fluctuations in the atmospheric boundary layer, *J. Fluid Mech.* **86**, 491–511 (1975).
11. M. M. Gibson and B. E. Launder, On the calculation of horizontal turbulent free shear flows under gravitational influence, *J. Heat Transfer* **98**, 81–87 (1976).
12. W. Rodi, Turbulence models for environmental problems, in *Prediction Methods for Turbulent Flows* (edited by W. Kollmann), pp. 259–349. McGraw-Hill, New York (1980).
13. M. Ljuboja and W. Rodi, Prediction of horizontal and vertical turbulent buoyant wall jets, *J. Heat Transfer* **103**, 343–349 (1981).
14. S. C. Lin and S. C. Lin, Study of strong temperature mixing in subsonic grid turbulence, *Physics Fluids* **16**, 1587–1598 (1973).
15. Z. Warhaft and J. L. Lumley, An experimental study of the decay of temperature fluctuations in grid-generated turbulence, *J. Fluid Mech.* **88**, 659–684 (1975).
16. C. Bèguier, I. Dekeyser and B. E. Launder, Ratio of scalar and velocity dissipation time scales in shear flow turbulence, *Physics Fluids* **21**, 307–310 (1978).
17. J. P. Holman, *Heat Transfer* (4th edn.), p. 503. McGraw-Hill, New York (1976).
18. B. E. Launder, Heat and Mass transport. In *Turbulence—Topics in Applied Physics* (edited by P. Bradshaw), Springer, Berlin (1976).
19. J. L. Lumley, Prediction methods for turbulent flows, a lecture series, Von Karman Institute, Belgium (1975).
20. O. Zeman and J. L. Lumley, Modeling buoyancy driven mixed layers, *J. Atmos. Sci.* **33**, 1974–1988 (1976).
21. G. R. Newman, B. E. Launder and J. L. Lumley, Modeling the behaviour of homogeneous scalar turbulence, *J. Fluid Mech.* **111**, 217–232 (1981).
22. S. B. Pope, Consistent modeling of scalars in turbulent flows, *Physics Fluids* **26**, 404–408 (1983).
23. O. Zeman, The dynamics of entrainment in the planetary boundary layer; a study in turbulence modeling and parameterization. Ph.D. thesis, Pennsylvania State University (1975).
24. H. A. Panofsky, The atmospheric boundary layer below 150 meters, *A. Rev. Fluid Mech.* **6**, 147–177 (1974).
25. M. E. Crawford and W. M. Kays, A program for numerical computation of two dimensional internal/external boundary flow, Report HMT 23, Stanford University California (1975).
26. B. J. Daly and F. H. Harlow, Transport equations in turbulence, *Physics Fluids* **13**, 2634–2649 (1970).
27. C. C. Shir, A preliminary number study of atmospheric turbulent flows in the idealized planetary boundary layer, *J. Atmos. Sci.* **30**, 1327–1339 (1973).
28. A. E. Perry and P. H. Hoffman, An experimental study of turbulent convective heat transfer from a flat plate, *J. Fluid Mech.* **77**, 355–368 (1976).
29. J. P. Schon, C. Rey, P. Mery and J. Mathieu, Experimental study of a turbulent stratified boundary layer developing on a rough plate, in *Heat Transfer and Turbulent Buoyant Convection*, (edited by D. B. Spalding and N. Afgan). Hemisphere, Washington D.C. (1977).

MODELE DE TURBULENCE A QUATRE EQUATIONS POUR LE CALCUL DE LA COUCHE LIMITE TURBULENTE SENSIBLE AUX FORCES D'ARCHIMEDE SUR UNE PLAQUE PLANE

Résumé—La convection thermique turbulente avec un effet important de force d'Archimède sur une plaque plane horizontale chauffée ou refroidie est numériquement analysée en résolvant quatre équations pour la variance de la température θ^2 , le taux de destruction ε_θ , l'énergie cinétique turbulente k et le taux de dissipation d'énergie ε . Le facteur temps-échelle R des fluctuations de température en relation avec les fluctuations de vitesse, défini par $(\overline{\theta^2}/\varepsilon_\theta)/(2k/\varepsilon)$ est trouvé varier fortement à travers la couche limite. Pour des conditions aussi bien fortement stables que fortement instables, le modèle à quatre équations fournit des résultats meilleurs sur le profil de température moyenne et sur le flux de chaleur que le modèle à deux équations. On trouve aussi que la valeur de la constante K_θ de Von Karman n'est pas une constante universelle mais qu'elle dépend de la stratification thermique de la couche limite.

TURBULENZ-MODELL MIT VIER GLEICHUNGEN FÜR DIE BERECHNUNG DER TURBULENTEN GRENZSCHICHT, DIE SICH BEI DER AUFTRIEBSSTRÖMUNG AN EINER EBENEN PLATTE EINSTELLT

Zusammenstellung—Der Wärmeübergang bei turbulenter Konvektion mit erheblichem Einfluß von Auftriebseffekten an einer beheizten oder gekühlten waagerechten ebenen Platte wird numerisch analysiert und zwar durch die Lösung von vier Gleichungen für die mittlere quadratische Temperaturvarianz $\bar{\theta}^2$, das Maß seiner Zerströung ϵ_θ , die turbulente kinetische Energie k und das Maß für die Dissipation der kinetischen Energie ϵ . Der turbulente Zeit-Maßstab R der Temperaturschwankungen relativ zu den Geschwindigkeitsschwankungen, definiert durch $(\bar{\theta}^2/\epsilon_\theta)/(2k/\epsilon)$, variiert sehr stark innerhalb der Grenzschicht. Unter sehr stabilen und sehr instabilen Bedingungen liefert das Modell mit vier Gleichungen bessere Ergebnisse für das mittlere Temperaturprofil und die Wärmestromdichte an der Oberfläche als das Modell mit zwei Gleichungen. Es ergab sich auch, daß die thermische von-Karman-Konstante keine universelle Konstante ist, sondern von der thermischen Schichtung der Grenzschicht abhängt.

СОСТОЯЩАЯ ИЗ ЧЕТЫРЕХ УРАВНЕНИЙ МОДЕЛЬ ТУРБУЛЕНТНОСТИ ДЛЯ РАСЧЕТА ТУРБУЛЕНТНОГО ПОГРАНИЧНОГО СЛОЯ С УЧЕТОМ ПОДЪЕМНОЙ СИЛЫ НАД ПЛОСКОЙ ПЛАСТИНОЙ

Аннотация—Турбулентный конвективный теплоперенос при существенном влиянии подъемной силы над нагреваемой или охлаждаемой горизонтальной плоской пластиной анализируется численно путем решения четырех уравнений, описывающих распределение среднеквадратичных значений пульсаций температуры $\bar{\theta}^2$, диссипации температурных пульсаций ϵ_θ , турбулентной кинетической энергии и диссипации кинетической энергии ϵ . Найдено, что величина $(\bar{\theta}^2/\epsilon_\theta)/(2k/\epsilon)$ изменяется значительно поперек пограничного слоя. Как для очень устойчивых, так и сильно неустойчивых условий модель четырех уравнений дает намного лучшие результаты для средних значений профиля температур и теплового потока на поверхности, чем модель из двух уравнений. Найдено также, что тепловая постоянная Кармана K_θ не является универсальной постоянной, а зависит от температурной стратификации пограничного слоя.